

# Induction of p21 protein protects against sulforaphane-induced mitotic arrest in LNCaP human prostate cancer cell line

Anna Herman-Antosiewicz,<sup>1</sup> Hui Xiao,<sup>2</sup>  
Karen L. Lew,<sup>2</sup> and Shivendra V. Singh<sup>2</sup>

<sup>1</sup>Department of Molecular Biology, University of Gdańsk, Gdańsk, Poland and <sup>2</sup>Department of Pharmacology and University of Pittsburgh Cancer Institute, University of Pittsburgh School of Medicine, Pittsburgh, Pennsylvania

## Abstract

Previous studies have indicated that D,L-sulforaphane (SFN), a synthetic cancer chemopreventive analogue of cruciferous vegetable-derived isomer (–)-1-isothiocyanato-(4R)-(methylsulfinyl)-butane, activates a checkpoint kinase 2 (Chk2)–dependent G<sub>2</sub>-M phase cell cycle arrest in p53-deficient human prostate cancer cells. Because p53 is a downstream target of Chk2 kinase and known to regulate G<sub>2</sub>-M transition by transcriptional regulation of cyclin-dependent kinase (Cdk) inhibitor p21<sup>Cip1/Waf1</sup> (p21), the present study was undertaken to determine the role of p21 in SFN-induced cell cycle arrest using wild-type p53–expressing cell line LNCaP. The SFN treatment caused a modest increase in S phase fraction and a marked increase in G<sub>2</sub>-M fraction in LNCaP cells in a concentration- and time-dependent manner. The SFN-induced S phase arrest correlated with a reduction in protein levels of cyclin D1, cyclin E, Cdk4, and Cdk6, whereas activation of the G<sub>2</sub>-M checkpoint was accompanied by induction of cyclin B1 and down-regulation of Cdk1 and Cdc25C protein levels. The SFN-treated LNCaP cells were also arrested in mitosis as revealed by immunofluorescence microscopy and increased Ser<sup>10</sup> phosphorylation of histone H3, a sensitive marker for mitotic cells. The SFN treatment increased activating phosphorylation of Chk2 (Thr<sup>68</sup>) that was accompanied by induction of p53 and p21. The SFN-induced mitotic arrest was statistically significantly

increased by small interfering RNA–based knockdown of p21. However, p21 protein knockdown did not have any appreciable effect on SFN-induced cytoplasmic histone-associated DNA fragmentation (apoptosis). In conclusion, the present study indicates that induction of p21 protects against SFN-induced mitotic arrest in LNCaP cells. [Mol Cancer Ther 2007;6(5):1673–81]

## Introduction

Epidemiologic studies continue to support the premise that dietary intake of cruciferous vegetables may lower the risk of different types of malignancies including prostate cancer (1–4). Anticarcinogenic effect of cruciferous vegetables is attributed to organic isothiocyanates, which are generated due to myrosinase-mediated hydrolysis of corresponding glucosinolates (5, 6). Broccoli is a rather rich source of the isothiocyanate compound (–)-1-isothiocyanato-(4R)-(methylsulfinyl)-butane (L-SFN). The L-SFN and its synthetic analogue D,L-sulforaphane (SFN) have generated a great deal of research interest due to their remarkable anticancer effects (7–14). For instance, L-SFN or SFN has been shown to afford significant protection against chemically induced cancer in animal models (8, 11–13). Cancer chemoprevention by L-SFN or SFN has been observed against 9,10-dimethyl-1,2-benzanthracene–induced mammary cancer in rats, azoxymethane-induced colonic aberrant crypt foci in rats, benzo[*a*]pyrene-induced forestomach cancer in mice, and 7,12-dimethylbenzo[*a*]anthracene/12-*O*-tetradecanoylphorbol 13-acetate–induced skin tumorigenesis in mice (8, 11–13). More recently, SFN administration was shown to significantly inhibit lung metastasis induced by B16F-10 melanoma cells in C57BL/6 mice (14).

Evidence is accumulating to indicate that SFN can suppress proliferation of cultured cancer cells by causing cell cycle arrest and apoptosis induction (15–24). Interestingly, normal epithelial cells, including a normal human prostate epithelial cell line PrEC and an immortalized normal human bronchial epithelial cell line BEAS-2B, are significantly more resistant to apoptosis induction by SFN compared with cancer cells (21). Consistent with these cellular results, oral administration of SFN significantly retards growth of PC-3 human prostate cancer xenografts in nude mice without causing weight loss or any other side effects (18). Inhibition of histone deacetylase activity by SFN has also been observed in human benign prostate hyperplasia epithelial cell line BPH-1 and PC-3 and LNCaP human prostate cancer cells (23).

An understanding of the mechanism(s) by which SFN causes cell cycle arrest and apoptosis induction is critical for its further clinical development because this knowledge

Received 12/28/06; revised 3/26/07; accepted 3/30/07.

Grant support: National Cancer Institute/USPHS grants CA115498 and CA101753.

The costs of publication of this article were defrayed in part by the payment of page charges. This article must therefore be hereby marked *advertisement* in accordance with 18 U.S.C. Section 1734 solely to indicate this fact.

Note: A. Herman-Antosiewicz and H. Xiao contributed equally to this work.

Requests for reprints: Shivendra V. Singh, 2.32A Hillman Cancer Center Research Pavilion, University of Pittsburgh Cancer Institute, 5117 Centre Avenue, Pittsburgh, PA 15213. Phone: 412-623-3263; Fax: 412-623-7828. E-mail: singhs@upmc.edu

Copyright © 2007 American Association for Cancer Research.

doi:10.1158/1535-7163.MCT-06-0807

could lead to identification of mechanism-based biomarkers potentially useful in future clinical trials. Recent studies have offered novel insights into the mechanism of SFN-induced apoptosis (15, 16, 18, 20–22, 24, 25). Studies have shown that SFN-induced apoptosis in human prostate cancer cells is initiated by reactive oxygen species and regulated by proapoptotic multidomain Bcl-2 family members Bax and Bak (20–22). More recently, we showed that SFN treatment causes autophagy in PC-3 and LNCaP cells, which protects against apoptosis by this agent (26). Despite these advances, however, signaling pathways responsible for SFN-induced cell cycle arrest are not fully defined.

Previous studies have revealed that SFN treatment causes G<sub>2</sub>-M phase cell cycle arrest in different cells including p53-deficient PC-3 cells (15, 19, 20, 23). We also found that the SFN-induced G<sub>2</sub>-M phase cell cycle arrest in PC-3 cells is caused by checkpoint kinase 2 (Chk2)-mediated phosphorylation of Cdc25C leading to its sequestration in the cytosol (19). The SFN-mediated cell cycle arrest in BPH-1 and PC-3/LNCaP cells correlates with induction of cyclin-dependent kinase (Cdk) inhibitor p21<sup>cip1/Waf1</sup> (p21; ref. 23), which is a transcriptional target of p53 tumor suppressor (27, 28). Because SFN treatment causes induction of p21 (23), it was of interest to investigate whether SFN-induced cell cycle arrest is influenced by p21 protein level. In the present study, we have addressed this question using wild-type p53-expressing cell line LNCaP. Here, we provide experimental evidence to indicate that induction of p21 protein protects against SFN-induced mitotic arrest in LNCaP cells.

## Materials and Methods

### Reagents

SFN (purity >98%) was purchased from LKT Laboratories. Penicillin/streptomycin antibiotic mixture, HEPES buffer solution, sodium pyruvate, and fetal bovine serum were from Invitrogen; RPMI 1640 was from Mediatech; propidium iodide and 4',6-diamidino-2-phenylindole were from Sigma; RNaseA was from Promega; and the reagents for electrophoresis were from Bio-Rad. The antibodies against cyclin B1, Cdk1, Cdc25C, cyclin D1, phosphorylated (Thr<sup>68</sup>)-Chk2, cyclin A, cyclin E, Cdk2, and Cdc25A were from Santa Cruz Biotechnology; the antibody against phosphorylated (Ser<sup>10</sup>)-histone H3 was from Upstate; the antibodies against actin and  $\alpha$ -tubulin were from Sigma; the antibodies against Cdc25B, p21, Cdk4, and Cdk6 were from BD Biosciences; and the antibodies against total p53 and phosphorylated (Ser<sup>15</sup>)-p53 were from Cell Signaling Technology.

### Cell Culture and Analysis of Cell Cycle Distribution

Monolayer cultures of LNCaP cells were obtained from the American Type Culture Collection and maintained in RPMI 1640 supplemented with 10% (v/v) non-heat-inactivated fetal bovine serum, HEPES, sodium pyruvate, 0.2% glucose, and antibiotics in a humidified atmosphere of 95% air and 5% CO<sub>2</sub>. The effect of SFN on cell cycle

distribution was determined by flow cytometry after staining the cells with propidium iodide. Briefly,  $5 \times 10^5$  cells were seeded in T25 flasks and allowed to attach by overnight incubation. The medium was replaced with fresh complete medium containing desired concentrations of SFN. Stock solution of SFN was prepared in DMSO, and an equal volume of DMSO (final concentration <0.1%) was added to the controls. After treatment for desired time period at 37°C, floating and adherent cells were collected, washed with PBS, and fixed with 70% ethanol. The cells were then treated with RNaseA and propidium iodide for 30 min, and the stained cells were analyzed using a Coulter Epics XL Flow Cytometer equipped with Expo 32 ADC Cytometer software (19).

### Immunoblotting

After treatment with DMSO (control) or desired concentrations of SFN for specified time periods, floating and attached cells were collected and lysed as described by us previously (19, 21). Lysate proteins were resolved by SDS-PAGE and transferred onto polyvinylidene fluoride membrane. Immunoblotting was done as described previously (19, 21). Change in protein level was determined by densitometric scanning of the immunoreactive bands and corrected for actin loading control.

### Immunofluorescence Microscopy

The LNCaP cells ( $2 \times 10^5$ ) were grown on coverslips and allowed to attach overnight. The cells were then exposed to DMSO or 20  $\mu$ mol/L SFN for 16 or 24 h at 37°C, washed with PBS, and fixed with 2% paraformaldehyde at 4°C overnight. The cells were permeabilized with 0.1% Triton X-100 for 15 min at room temperature, washed with PBS, and incubated with a solution containing bovine serum albumin (BSA) and 0.15% (w/v) glycine (BSA buffer) for 1 h at room temperature. The cells were incubated with anti- $\alpha$ -tubulin antibody (1:4,000 dilution in BSA buffer) for 1 h at room temperature. Cells were then washed with BSA buffer and incubated with 1  $\mu$ g/mL Alexa Fluor 568-conjugated goat anti-mouse antibody (Molecular Probes) for 1 h at room temperature followed by counterstaining with 10 ng/mL 4',6-diamidino-2-phenylindole. Slides were mounted and examined under a Leica fluorescence microscope at  $\times 100$  (objective lens) magnification. The mitotic figures with condensed chromatin were counted. A total of 300 cells were scored in duplicate.

### Knockdown of p21 and p53 Protein

SignalSilence p21-targeted small interfering RNA (siRNA) was purchased from Cell Signaling Technology, and a control nonspecific siRNA was procured from Qiagen. RNA interference of p53 was done using p53 specific siRNA duplexes (Santa Cruz Biotechnology). For transfection, LNCaP cells were seeded in six-well plates and transfected at 30% confluency with 100 nmol/L siRNA using oligofectamine according to the manufacturer's recommendations. After 24 to 36 h, cells were treated with 20  $\mu$ mol/L SFN or DMSO (control) for 12 or 24 h. Both floating and adherent cells were collected, washed with PBS, and processed for analysis of cell cycle distribution, determination of histone H3 phosphorylation,

immunoblotting, or analysis of cytoplasmic histone-associated DNA fragmentation as described previously (19, 21, 22).

### Flow Cytometric Analysis of Ser<sup>10</sup> Phosphorylated Histone H3

The effect of SFN treatment on Ser<sup>10</sup> phosphorylation of histone H3 was determined by flow cytometry by the method of Widrow and Laird (29), with some modifications described by us previously (30). Briefly, the cells were treated with SFN as described above, fixed in 70% ethanol at 4°C, suspended in 1 mL of 0.25% Triton X-100 in PBS, and incubated on ice for 15 min. The cells were collected, suspended in 100 µL of PBS containing 1% BSA and 0.75 µg of a polyclonal anti-phosphorylated (Ser<sup>10</sup>)-histone H3 antibody, and incubated at 4°C overnight with gentle shaking. The cells were then rinsed with PBS containing 1% BSA and incubated in the dark with FITC-conjugated goat anti-rabbit antibody (1:50 dilution in PBS containing 1% BSA) for 30 min at room temperature. The cells were washed with PBS containing 1% BSA and treated with RNaseA and propidium iodide for 30 min. Cellular fluorescence was measured by a Coulter Epics XL Flow Cytometer.

## Results

### SFN Treatment Caused G<sub>2</sub>-M Phase Cell Cycle Arrest in LNCaP Cells

We have shown previously that proliferation of LNCaP cells is decreased significantly by a 24-h exposure to 10, 20, and 40 µmol/L SFN (24). Initially, we designed experiments to determine whether SFN-mediated suppression of LNCaP cell proliferation correlates with cell cycle arrest. As can be seen in Fig. 1, a 24-h treatment of LNCaP cells with 10, 20, or 40 µmol/L SFN resulted in a modest yet statistically significant S phase arrest and a marked G<sub>2</sub>-M phase arrest that was accompanied by a decrease in G<sub>0</sub>-G<sub>1</sub> phase cells. On the other hand, a similar treatment of LNCaP cells with 60 µmol/L SFN resulted in a statistically significant increase in sub-diploid fraction, indicating apoptosis induction.

In time course experiments using 20 µmol/L SFN, a modest increase in S phase fraction was evident 24 h posttreatment and maintained for at least up to 48 h (Table 1). Interestingly, the SFN-mediated accumulation of G<sub>2</sub>-M phase cells was evident as early as 4 h after treatment and peaked between 12 and 24 h after drug exposure. There was an increase of control cells in G<sub>0</sub>-G<sub>1</sub> phase over time with a concomitant decrease in S phase fraction (Table 1) possibly due to reaching confluency by cells especially at 36- to 48-h time points. A statistically significant increase in sub-diploid fraction (apoptotic cells) in SFN-treated LNCaP cultures compared with DMSO-treated control cells was observed at 24 h time point and increased gradually with increasing exposure time (Table 1). These results indicated that SFN-treated LNCaP cells were mainly arrested in the G<sub>2</sub>-M phase of the cell cycle, and that higher SFN concentrations caused accumulation of sub-diploid (apoptosis) fraction.

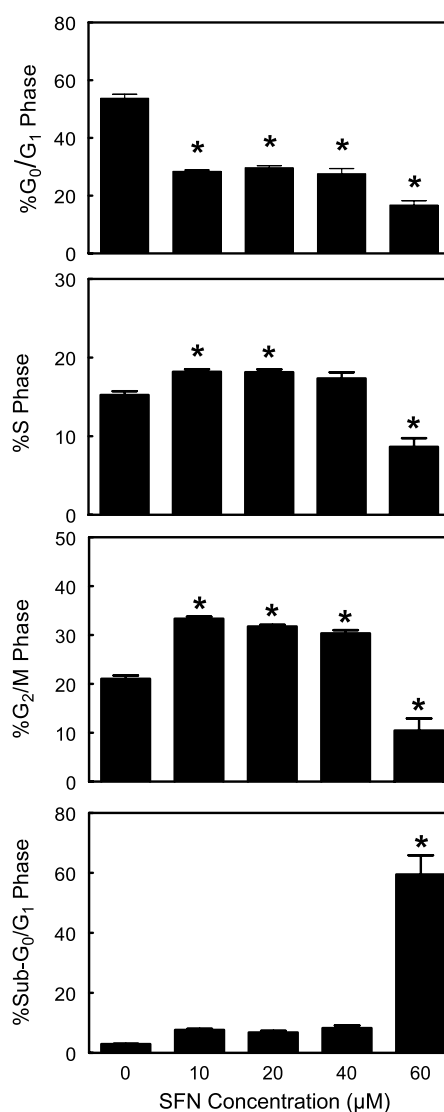


**Figure 1.** Percentage of cells in different phases of the cell cycle in LNCaP cultures treated for 24 h with DMSO (control) or the indicated concentrations of SFN. Similar results were observed in two independent experiments. Columns, mean ( $n = 3$ ); bars, SE. \*,  $P < 0.05$ , significantly different compared with DMSO-treated control by one-way ANOVA followed by Dunnett's test.

### Effect of SFN Treatment on Levels of G<sub>1</sub>-S and G<sub>2</sub>-M Specific Cyclins and Cdks

Next, we proceeded to determine the mechanism by which SFN treatment may cause S and G<sub>2</sub>-M phase cell cycle arrest in LNCaP cells. Eukaryotic cell cycle progression involves sequential activation of Cdks, whose activity is dependent upon their association with corresponding regulatory cyclins (31, 32). For instance, completion of S phase and progression through G<sub>2</sub> requires activation of cyclin A/Cdk2 and cyclin A/Cdk1 complexes (31, 32). At the same time, the G<sub>1</sub>-S transition is regulated by complexes formed by cyclin D1, Cdk4, Cdk6 and cyclin E and Cdk2 (31, 32). Activation of Cdk/cyclin kinase complex

**Table 1. Time course kinetics of SFN-induced cell cycle arrest in LNCaP cells**

Group	Time (h)	Percent cells in the following phases			
		Sub-G <sub>0</sub> -G <sub>1</sub>	G <sub>0</sub> -G <sub>1</sub>	S	G <sub>2</sub> -M
Control	4	2 ± 0.9	48 ± 0.1	20 ± 0.5	29 ± 0.6
SFN	4	1 ± 0.1	42 ± 0.4*	22 ± 0.3	33 ± 0.6*
Control	8	2 ± 0.5	63 ± 0.4	18 ± 0.4	17 ± 1.1
SFN	8	2 ± 0.4	40 ± 0.7*	15 ± 0.3	40 ± 0.2*
Control	12	1 ± 0.3	61 ± 0.8	12 ± 0.2	23 ± 0.9
SFN	12	2 ± 0.2	35 ± 0.5*	16 ± 0.6	43 ± 0.6*
Control	24	2 ± 0.0	51 ± 0.7	14 ± 0.2	24 ± 0.2
SFN	24	9 ± 0.8*	31 ± 1.5*	17 ± 0.3*	33 ± 1.0*
Control	36	2 ± 0.3	60 ± 0.7	11 ± 0.2	20 ± 0.1
SFN	36	13 ± 0.1*	39 ± 1.1*	16 ± 0.8*	25 ± 0.0*
Control	48	2 ± 1.1	66 ± 0.8	9 ± 0.4	18 ± 0.6
SFN	48	17 ± 2.1*	34 ± 0.8*	16 ± 0.3*	27 ± 1.3*

NOTE: Percentage of cells in different phases of the cell cycle in LNCaP cultures treated with DMSO (control) or 20  $\mu\text{mol/L}$  SFN for the indicated time periods. The short- and long-term time course kinetics studies were performed separately. Similar results were observed in two independent experiments. Results are mean  $\pm$  SE ( $n = 2-3$ ).

\*Significantly different ( $P < 0.05$ ) compared with DMSO-treated control by paired  $t$  test.

is mediated by Cdc25 family of dual specificity phosphatases (33). Immunoblotting data for the effect of SFN treatment on levels of G<sub>1</sub>-S specific cyclins and Cdks are summarized in Fig. 2A. The levels of the cyclins and Cdks necessary for G<sub>1</sub>-S transition (cyclin D1, cyclin E, Cdk4, and Cdk6) were reduced markedly on treatment of LNCaP cells with 20  $\mu\text{mol/L}$  SFN (Fig. 2A), although with different kinetics. For instance, the SFN-mediated reduction in cyclin D1 protein level was observed as early as 1 h after drug exposure (about 50% reduction compared with control at 1 h time point as determined by densitometric scanning of the immunoreactive bands and corrected for actin loading control), whereas a marked decrease in the levels of cyclin E and Cdk4 proteins became evident only at 8- to 24-h time points (Fig. 2A). Interestingly, the level of Cdk2 protein was increased on treatment of LNCaP cells with 20  $\mu\text{mol/L}$  SFN. For example, the level of Cdk2 protein was increased by about 1.6- to 2.0-fold in LNCaP cells treated with SFN for 4 to 24 h (Fig. 2A). Although the level of cyclin A protein was increased slightly on treatment of LNCaP cells with 20  $\mu\text{mol/L}$  SFN for 16 and 24 h (about 40% increase compared with DMSO-treated control), SFN treatment did not have any appreciable effect on Cdc25A protein level (data not shown). These results indicated that the SFN-induced S phase arrest was accompanied by a decrease in protein levels of cyclin D1, cyclin E, Cdk4, and Cdk6.

A complex between Cdk1 and cyclin B1 is important for entry into mitosis in most organisms (31, 32). The Cdk1/cyclin B1 complex is retained in an inactive state by reversible phosphorylation at Thr<sup>14</sup> and Tyr<sup>15</sup> of Cdk1 (31, 32). Dephosphorylation of Cdk1, and hence activation of Cdk1/cyclin B1 kinase complex, is catalyzed by Cdc25B and Cdc25C, and this reaction is believed to be a rate-

limiting step for entry into mitosis (33). Immunoblotting data for the effect of SFN treatment on levels of proteins involved in regulation of G<sub>2</sub>-M transition are summarized in Fig. 2B. SFN treatment caused a marked increase in the protein level of cyclin B1 that was evident as early as 4 h after treatment. In addition, the SFN-mediated induction of cyclin B1 protein was maintained for the duration of the experiment (24 h posttreatment). The levels of Cdk1 and Cdc25C proteins were reduced markedly in SFN-treated LNCaP cells at 8- to 24-h time points, although a modest increase in Cdc25C protein level relative to control was noticeable at 1- to 4-h time points. The SFN treatment modestly increased the level of Cdc25B protein at 1- to 4-h time points (Fig. 2B). These results suggested that SFN treatment might cause inactivation of Cdk1 possibly due to a reduction in the levels of Cdk1 and Cdc25C proteins.

#### SFN Treatment Caused Mitotic Arrest in LNCaP Cells

In cycling cells, cyclin B1 protein level increases abruptly as the cells acquire 4N DNA content, peaks during the metaphase/anaphase transition, and declines precipitously upon completion of mitosis (34-36). Because there was a marked increase in protein level of cyclin B1 (Fig. 2B), we reasoned that SFN-treated LNCaP cells might be arrested in mitosis. We explored this possibility by immunofluorescence microscopy following staining of control (DMSO for 16 or 24 h) and SFN-treated (20  $\mu\text{mol/L}$  for 16 or 24 h) LNCaP cells with anti- $\alpha$ -tubulin antibody and 4',6-diamidino-2-phenylindole. As shown in Fig. 3A, the DMSO-treated control cells exhibited intact microtubule network. The tubulin network in a large fraction of SFN-treated LNCaP cells was disrupted, and the staining was restricted to the periphery of the nucleus. In addition, the fraction of mitotic cells with condensed chromatin was markedly higher in SFN-treated LNCaP cultures at both 16- and 24-h time points compared with vehicle-treated control (Fig. 3A). The SFN-induced mitotic block in LNCaP cells was confirmed by analysis of Ser<sup>10</sup> phosphorylation of histone H3, which has emerged as a sensitive marker for mitotic cells (37). The Ser<sup>10</sup> phosphorylation of histone H3 begins in prophase, peaks during metaphase, and declines during anaphase (38, 39). Agents initiating premature chromosome condensation have been shown to increase Ser<sup>10</sup> phosphorylation of histone H3 (40, 41). As can be seen in Fig. 3B, the Ser<sup>10</sup> phosphorylation of histone H3 was very low in control cells but clearly evident in SFN-treated LNCaP cells as judged by flow cytometry (Fig. 3B). The SFN-mediated Ser<sup>10</sup> phosphorylation of histone H3 was also evident in immunoblotting experiment (Fig. 3C). These results indicated that SFN treatment caused mitotic arrest in LNCaP cells.

#### SFN Treatment Caused Induction of p21 Protein in LNCaP Cells

We have shown previously that SFN treatment causes activation of Chk2, leading to Ser<sup>216</sup> phosphorylation of Cdc25C and ultimately G<sub>2</sub>-M phase cell cycle arrest in p53-deficient PC-3 cells (19). To address the question of whether the correlation between SFN-mediated Chk2 activation and

cell cycle arrest is unique to PC-3 cells, we determined the effect of SFN treatment (20  $\mu\text{mol/L}$ ) on activating phosphorylation (Thr<sup>68</sup>) of Chk2 in LNCaP cells by immunoblotting, and the results are shown in Fig. 4. The Chk2 kinase is an intermediary of DNA damage checkpoints and activated in response to various stimuli including ionizing radiation and UV irradiation (42–44). As can be seen in Fig. 4, SFN treatment caused a rapid and sustained increase in Thr<sup>68</sup> phosphorylation of Chk2. Because both Cdc25C and p53 are downstream targets of Chk2 (27), it was of interest to determine whether SFN treatment caused phosphorylation of these proteins in LNCaP cells. Unlike PC-3 cells, SFN treatment did not have any appreciable effect on level of phosphorylated (Ser<sup>216</sup>)-Cdc25C (results not shown). On the other hand, the levels of total p53 and phosphorylated (Ser<sup>15</sup>)-p53 were increased markedly on treatment of LNCaP cells with 20  $\mu\text{mol/L}$  SFN especially at 8- to 24-h time points (Fig. 4). Next, we explored the possibility of whether SFN-mediated induction of p53 was accompanied by induction of its transcriptional target p21. Indeed, SFN-treated LNCaP cells exhibited a marked increase in the level of p21 protein that occurred before changes in p53 protein level and phosphorylation. For instance, a marked increase in protein level of p53 (about 2.6-fold increase over control) was not observed until 8 h

after treatment, but SFN-mediated induction of p21 was evident even after 2 h of treatment (Fig. 4). These results pointed toward a p53-independent mechanism in SFN-mediated induction of p21.

#### Depletion of p21 Protein Level Increased SFN-induced Mitotic Arrest

Next, we proceeded to determine whether p21 induction affected SFN-induced cell cycle arrest. Transient transfection of LNCaP cells with a p21-targeted siRNA resulted in near complete loss of p21 protein (Fig. 5A). The effect of SFN treatment on cell cycle distribution was determined by flow cytometry, and the results are summarized in Fig. 5B and C. Similar to untransfected cells, treatment with 20  $\mu\text{mol/L}$  SFN resulted in a modest increase in S phase fraction in control siRNA transfected cells (Fig. 5B). The SFN-induced S phase arrest was also observed in p21-depleted LNCaP cells. Similarly, SFN-mediated G<sub>2</sub>-M phase cell cycle arrest was evident in cells transfected with control siRNA as well as p21-targeted siRNA (Fig. 5C). However, the G<sub>2</sub>-M phase cell cycle arrest caused by SFN was relatively more pronounced in p21-depleted LNCaP cells compared with control siRNA-transfected cells (Fig. 5C). These results suggested that p21 protein depletion might promote SFN-mediated mitotic arrest that is unlikely to be reflected in analysis of total G<sub>2</sub>-M fraction

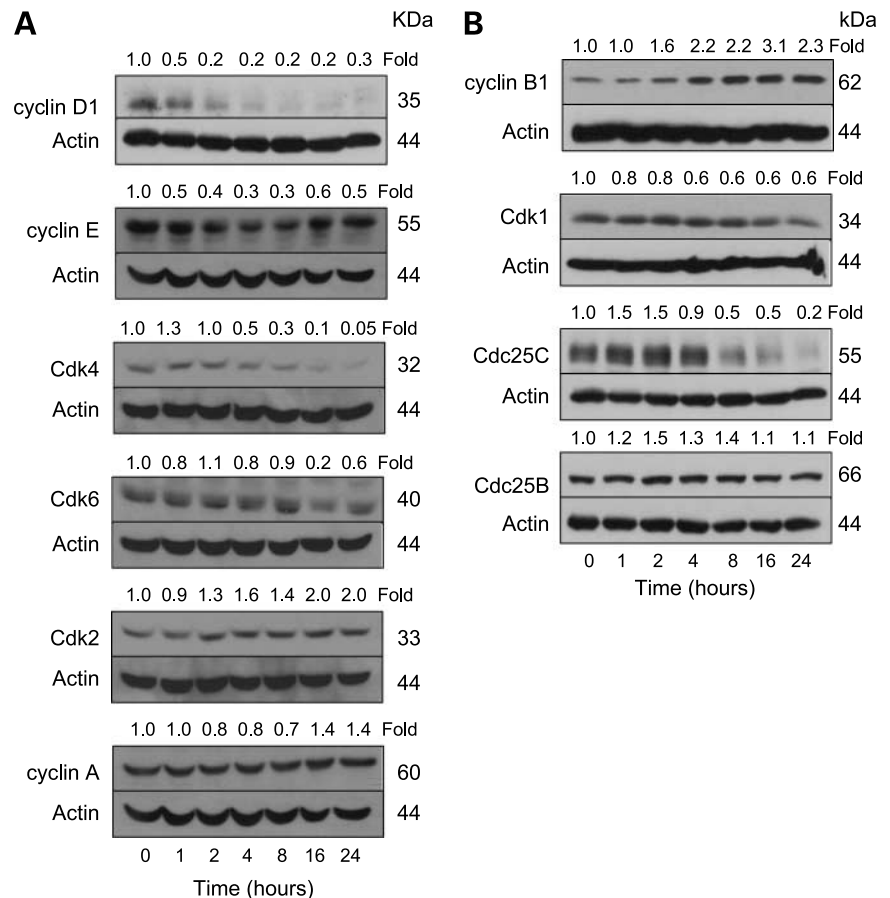


**Figure 2.** **A**, immunoblotting for cyclin D1, cyclin E, Cdk4, Cdk6, Cdk2, and cyclin A using lysates from LNCaP cells treated with 20  $\mu\text{mol/L}$  SFN for the indicated time periods. **B**, immunoblotting for cyclin B1, Cdk1, Cdc25C, and Cdc25B using lysates from LNCaP cells treated with 20  $\mu\text{mol/L}$  SFN for the indicated time periods. The blots were stripped and reprobbed with anti-actin antibody to normalize for differences in protein loading. Numbers on top of the bands, changes in protein levels relative to control as determined by densitometric scanning of the immunoreactive bands and corrected for actin loading control.

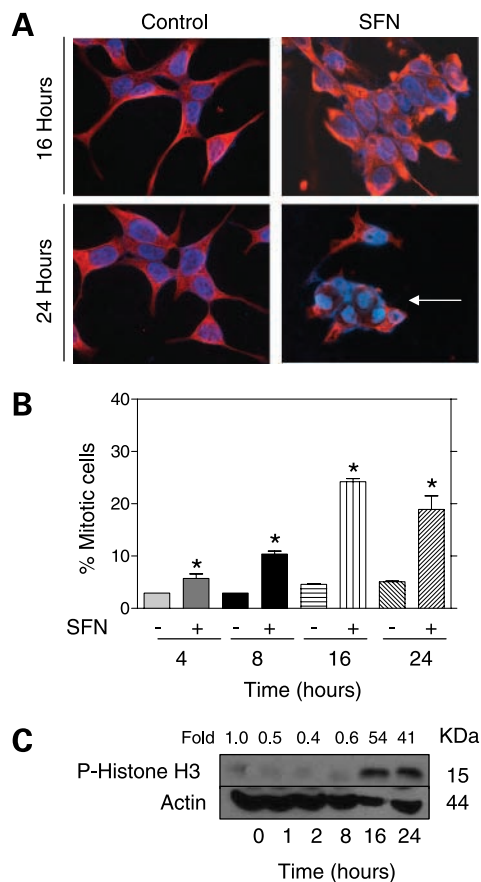


**Figure 3.** **A**, fluorescence microscopy depicting  $\alpha$ -tubulin (red) and chromatin (blue) staining in LNCaP cultures treated for 16 or 24 h with DMSO (control) or 20  $\mu$ mol/L SFN. Note disruption of the tubulin network and accumulation of mitotic cells with condensed chromatin in SFN treated LNCaP cultures. Similar results were observed in replicate experiments. **B**, flow cytometric analysis of phosphorylated (Ser<sup>10</sup>)-histone H3 levels in LNCaP cultures following treatment with DMSO (control) or 20  $\mu$ mol/L SFN for the indicated time periods. Columns, mean ( $n = 3$ ); bars, SE. \*,  $P < 0.05$ , significantly different compared with DMSO-treated control by paired  $t$  test. **C**, immunoblotting for phosphorylated (Ser<sup>10</sup>)-histone H3 (*P-Histone H3*) using lysates from LNCaP cells treated with 20  $\mu$ mol/L SFN for the indicated time periods. The blot was stripped and reprobbed with anti-actin antibody to normalize for differences in protein loading. Immunoblotting was done twice using independently prepared lysates, and the results were similar. Numbers on top of the bands, changes in protein levels relative to control as determined by densitometric scanning of the immunoreactive bands and corrected for actin loading control.

by flow cytometry. To test this possibility, we compared Ser<sup>10</sup> phosphorylation of histone H3 by flow cytometry in LNCaP cells transiently transfected with a control nonspecific siRNA and p21-targeted siRNA and treated for 24 h with either DMSO (control) or 20  $\mu$ mol/L SFN. As can be seen in Fig. 5D, the SFN-mediated increase in Ser<sup>10</sup> phosphorylation of histone H3 was statistically significantly more pronounced in p21-depleted cells compared with cells transfected with control siRNA (Fig. 5D). Collectively, these results indicated that p21 protein depletion increased SFN-induced mitotic arrest in LNCaP cells.

We also considered an alternate hypothesis that SFN-mediated induction of p21 may increase apoptosis especially in cells arrested in mitosis. This hypothesis would be substantiated if knockdown of p21 protein level decreases the number of cells undergoing apoptosis. To systematically explore this possibility, we determined the effect of p21 protein knockdown on SFN-induced apoptosis by monitoring cytoplasmic histone-associated DNA fragmentation (a reliable and sensitive method for quantitation of apoptosis). Knockdown of p21 protein level did not have any appreciable effect on SFN-induced apoptosis (results not shown), thus arguing against this possibility.

We proceeded to determine the effect of p53 protein knockdown by using a p53-targeted siRNA to test whether expression of wild-type p53 influenced SFN-induced mitotic arrest. The SFN-induced mitotic arrest was maintained in LNCaP cells even after >90% knockdown of the p53 protein level (results not shown). Moreover, the extent of mitotic arrest resulting from a 16-h treatment with 20  $\mu$ mol/L SFN did not differ significantly between control nonspecific siRNA-transfected LNCaP cells and cells transfected with a p53-targeted siRNA (results not shown). These results indicated that the SFN-mediated mitotic arrest in LNCaP cells was independent of p53 expression.

## Discussion

The present study reveals that exposure of LNCaP cells to growth suppressive (24) and pharmacologically achievable

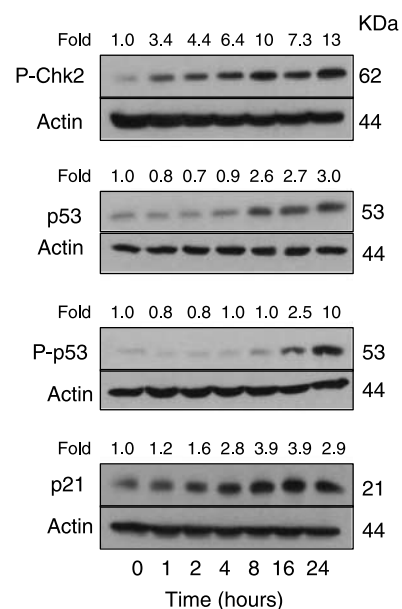


**Figure 4.** Immunoblotting for phosphorylated (Thr<sup>68</sup>)-Chk2 (*P-Chk2*), total p53, phosphorylated (Ser<sup>15</sup>)-p53 (*P-p53*), and p21 using lysates from LNCaP cells treated with 20  $\mu$ mol/L SFN for the indicated time periods. The blots were stripped and reprobbed with anti-actin antibody to normalize for differences in protein loading. Immunoblotting for each protein was done at least twice using independently prepared lysates, and the results were consistent. Numbers on top of the bands, changes in protein levels relative to control as determined by densitometric scanning of the immunoreactive bands and corrected for actin loading control.

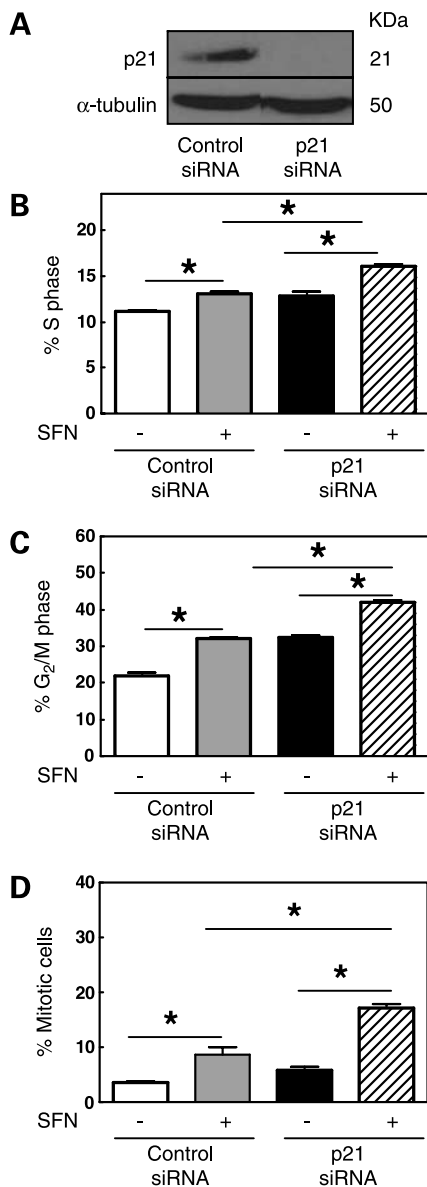


**Figure 5.** **A**, immunoblotting for p21 protein using lysates from LNCaP cells transiently transfected with a control nonspecific siRNA or p21-targeted siRNA. The blot was stripped and reprobed with anti- $\alpha$ -tubulin antibody to ensure equal protein loading. **B**, percentages of S phase fraction in LNCaP cells transiently transfected with control siRNA or p21-specific siRNA and treated for 12 h with DMSO (control) or 20  $\mu$ mol/L SFN. **C**, percentages of G<sub>2</sub>-M phase fraction in LNCaP cells transiently transfected with control siRNA and p21-specific siRNA and treated for 12 h with DMSO (control) or 20  $\mu$ mol/L SFN. **D**, percentage of mitotic cells with increased levels of phosphorylated (Ser<sup>10</sup>)-histone H3 (determined by flow cytometry) in LNCaP cultures transiently transfected with control siRNA or p21-specific siRNA and treated for 24 h with DMSO (control) or 20  $\mu$ mol/L SFN. Columns, mean ( $n = 3$ ); bars, SE. \*,  $P < 0.05$ , significantly different between the indicated groups by one-way ANOVA followed by Bonferroni's multiple comparison test.

concentrations of SFN (45) results in a modest S phase arrest but a marked G<sub>2</sub>-M phase cell cycle arrest in a time-dependent manner (Table 1). The S phase arrest is modest following treatment of LNCaP cells with SFN for 24 and

36 h (21–45% increase in percentage of S fraction over DMSO-treated control), but this cellular response is relatively more pronounced at the 48-h time point as evidenced by about 77% increase in S fraction in SFN-treated cells compared with DMSO-treated control (Table 1). On the other hand, the SFN-mediated G<sub>2</sub>-M phase cell cycle arrest is rapid and evident as early as 4 h posttreatment. The G<sub>2</sub>-M phase cell cycle arrest by SFN treatment at concentrations within the range used in the present study has also been observed in other cellular systems including HT29 human colon cancer cell line (15), F3II mouse sarcomatoid mammary carcinoma cell line (17), PC-3 and DU145 human prostate cancer cells (19, 20), and human benign prostate hyperplasia epithelial cell line BPH-1 (23). In contrast, previous studies by Chiao et al. (46) have documented a G<sub>1</sub> phase cell cycle arrest in LNCaP cells following a 24-h exposure to 3 and 9  $\mu$ mol/L SFN. In a follow-up study, the same group of investigators reported enrichment of G<sub>1</sub> fraction in DU145 human prostate cancer cells under similar conditions of SFN treatment (47), which is in sharp contrast to the G<sub>2</sub>-M phase arrest observed by Cho et al. (20) in the same cell line (10  $\mu$ mol/L SFN for 24 h). Discrepancy in cell cycle responses to SFN has also been reported in HT29 human colon cancer cells (15, 48). The reasons for discrepancy in cell cycle effects of SFN remain to be explained. Nonetheless, cell cycle perturbation seems to be an important mechanism in cancer cell growth inhibition by SFN (15, 17, 19, 20, 23, 46–50). It is interesting to note that despite a marked decrease in the protein levels of cyclin D1, cyclin E, Cdk4, and Cdk6 (Fig. 2A), SFN-treated LNCaP cells are able to enter the S phase. Because degradation of the G<sub>1</sub>-specific cyclins is necessary for cells to enter the S phase, it is reasonable to conclude that the decrease in G<sub>1</sub>-specific cyclins in our model is probably a consequence of progression beyond G<sub>1</sub> rather than the cause for S phase arrest.

The SFN-mediated G<sub>2</sub>-M phase cell cycle arrest in LNCaP cells correlates with an increase in cyclin B1 protein level and down-regulation of Cdk1 and Cdc25C protein levels (Fig. 2B). Although the mechanism of cell cycle arrest was not thoroughly investigated, induction of cyclin B1 upon treatment with SFN has also been documented in HT29 human colon cancer cells (15). We have shown previously that the SFN-mediated accumulation of G<sub>2</sub>-M fraction in PC-3 cells is accompanied by a decrease in protein levels of cyclin B1, Cdc25C, and Cdc25B and increased Chk2-dependent Ser<sup>216</sup> phosphorylation of Cdc25C (19). Although SFN treatment causes activation of Chk2 in LNCaP cells as evidenced by an increase in the level of phosphorylated (Thr<sup>68</sup>)-Chk2 (Fig. 4), the Ser<sup>216</sup> phosphorylation of Cdc25C is not increased in these cells (data not shown). These results suggest that the mechanism of SFN-induced G<sub>2</sub>-M phase arrest is probably cell line specific. It is possible that a decrease in the protein level of Cdc25C, which is a critical regulator of G<sub>2</sub>-M transition in eukaryotic cells (33) and observed in both PC-3 (19) and LNCaP cells (present study), is sufficient to trigger G<sub>2</sub>-M phase checkpoint activation even in the absence of Cdc25C phosphorylation.

This conclusion is consistent with our previous findings in PC-3 cells because abrogation of Ser<sup>216</sup> phosphorylation of Cdc25C by Chk2 protein knockdown offers only partial protection against SFN-induced G<sub>2</sub>-M arrest (19).

Degradation of cyclin B1 is necessary for cells to exit mitosis (34–36). The SFN treatment causes a marked increase in the level of cyclin B1 protein in LNCaP cells, suggesting that cells may escape G<sub>2</sub> arrest but are arrested in mitosis. Indeed, the immunofluorescence microscopy of SFN-treated LNCaP cells after staining with 4',6-diamidino-2-phenylindole as well as analysis of Ser<sup>10</sup> phosphorylation of histone H3 confirms mitotic arrest in our model. The SFN-mediated mitotic arrest is not restricted to the LNCaP cell line because similar response has been described previously in F3II mouse mammary carcinoma cells (17). Exposure of synchronized F3II cells to 15 μmol/L SFN results in elevated numbers of prophase/prometaphase mitotic figures, indicating progression beyond G<sub>2</sub> and arrest early in mitosis (17). Increased Ser<sup>10</sup> phosphorylation of histone H3 coupled with induction of cyclin B1 level on treatment with SFN has also been observed in MIA PaCa-2 pancreatic cancer cells (50). However, the precise mechanism by which SFN inhibits mitotic exit remains to be elucidated.

The present study reveals that SFN treatment causes induction of Cdk inhibitor p21 in LNCaP cells (Fig. 4). Although induction of p21 protein by SFN treatment has been observed previously in other cellular systems (23, 48), studies were lacking that could directly test the role of this protein in regulation of SFN-mediated cell cycle arrest. The present study points toward an important role of p21 in regulation of SFN-mediated cell cycle arrest. We show, for the first time, that knockdown of p21 protein potentiates SFN-induced mitotic arrest in LNCaP cells (Fig. 5). However, the SFN-mediated induction of p21 in our model seems independent of p53 because the increase in p21 level is observed even in the absence of p53 induction and Ser<sup>15</sup> phosphorylation (Fig. 4). Moreover, knockdown of p53 protein level does not have any appreciable effect on SFN-induced mitotic arrest. These results are consistent with the conclusions drawn by Myzak et al. (23), who have postulated that SFN-mediated induction of p21 is independent of p53 but probably linked to inhibition of histone deacetylase activity. Nonetheless, the present study provides experimental evidence to indicate that induction of p21 protein protects against SFN-mediated mitotic arrest.

## References

- Verhoeven DT, Goldbohm RA, van Poppel G, Verhagen H, van den Brandt PA. Epidemiological studies on *Brassica* vegetables and cancer risk. *Cancer Epidemiol Biomarkers Prev* 1996;5:733–48.
- Cohen JH, Kristal AR, Stanford JL. Fruit and vegetable intakes and prostate cancer risk. *J Natl Cancer Inst* 2000;92:61–8.
- Zhang SM, Hunter DJ, Rosner BA, et al. Intakes of fruits, vegetables, and related nutrients and the risk of non-Hodgkin's lymphoma among women. *Cancer Epidemiol Biomarkers Prev* 2000;9:477–85.
- Ambrosone CB, McCann SE, Freudenheim JL, Marshall JR, Zhang Y, Shields PG. Breast cancer risk in premenopausal women is inversely associated with consumption of broccoli, a source of isothiocyanates, but is not modified by GST genotype. *J Nutr* 2004;134:1134–8.
- Hecht SS. Inhibition of carcinogenesis by isothiocyanates. *Drug Metab Rev* 2000;32:395–411.
- Conaway CC, Yang YM, Chung FL. Isothiocyanates as cancer chemopreventive agents: their biological activities and metabolism in rodents and humans. *Curr Drug Metab* 2002;3:233–55.
- Zhang Y, Talalay P, Cho CG, Posner GH. A major inducer of anticarcinogenic protective enzymes from broccoli: isolation and elucidation of structure. *Proc Natl Acad Sci U S A* 1992;89:2399–403.
- Zhang Y, Kensler TW, Cho CG, Posner GH, Talalay P. Anticarcinogenic activities of sulforaphane and structurally related synthetic norbornyl isothiocyanates. *Proc Natl Acad Sci U S A* 1994;91:3147–50.
- Barcelo S, Gardiner JM, Gescher A, Chipman JK. CYP2E1-mediated mechanism of anti-genotoxicity of the broccoli constituent sulforaphane. *Carcinogenesis* 1996;17:277–82.
- Brooks JD, Paton VG, Vidanes G. Potent induction of phase 2 enzymes in human prostate cells by sulforaphane. *Cancer Epidemiol Biomarkers Prev* 2001;10:949–54.
- Chung FL, Conaway CC, Rao CV, Reddy BS. Chemoprevention of colonic aberrant crypt foci in Fischer rats by sulforaphane and phenethyl isothiocyanate. *Carcinogenesis* 2000;21:2287–91.
- Fahey JW, Haristoy X, Dolan PM, et al. Sulforaphane inhibits extracellular, intracellular, and antibiotic-resistant strains of *Helicobacter pylori* and prevents benzo[a]pyrene-induced stomach tumors. *Proc Natl Acad Sci U S A* 2002;99:7610–5.
- Gills JJ, Jeffery EH, Matusheski NV, Moon RC, Lantvit DD, Pezzuto JM. Sulforaphane prevents mouse skin tumorigenesis during the stage of promotion. *Cancer Lett* 2006;236:72–9.
- Thejass P, Kuttan G. Antimetastatic activity of sulforaphane. *Life Sci* 2006;78:3043–50.
- Gamet-Payraastre L, Li P, Lumeau S, et al. Sulforaphane, a naturally occurring isothiocyanate, induces cell cycle arrest and apoptosis in HT29 human colon cancer cells. *Cancer Res* 2000;60:1426–33.
- Misiewicz I, Skupinska K, Kasprzycka-Guttman T. Sulforaphane and 2-oxohexyl isothiocyanate induce cell growth arrest and apoptosis in L-1210 leukemia and ME-18 melanoma cells. *Oncol Rep* 2003;10:2045–50.
- Jackson SJT, Singletary KW. Sulforaphane: a naturally occurring mammary carcinoma mitotic inhibitor, which disrupts tubulin polymerization. *Carcinogenesis* 2004;25:219–27.
- Singh AV, Xiao D, Lew KL, Dhir R, Singh SV. Sulforaphane induces caspase-mediated apoptosis in cultured PC-3 human prostate cancer cells and retards growth of PC-3 xenografts *in vivo*. *Carcinogenesis* 2004;25:83–90.
- Singh SV, Herman-Antosiewicz A, Singh AV, et al. Sulforaphane-induced G<sub>2</sub>/M phase cell cycle arrest involves checkpoint kinase 2 mediated phosphorylation of Cdc25C. *J Biol Chem* 2004;279:25813–22.
- Cho S, Li G, Hu H, et al. Involvement of c-Jun N-terminal kinase in G<sub>2</sub>/M arrest and caspase-mediated apoptosis induced by sulforaphane in DU145 prostate cancer cells. *Nutr Cancer* 2005;52:213–24.
- Choi S, Singh SV. Bax and Bak are required for apoptosis induction by sulforaphane, a cruciferous vegetable derived cancer chemopreventive agent. *Cancer Res* 2005;65:2035–43.
- Singh SV, Srivastava SK, Choi S, et al. Sulforaphane-induced cell death in human prostate cancer cells is initiated by reactive oxygen species. *J Biol Chem* 2005;280:19911–24.
- Myzak MC, Hardin K, Wang R, Dashwood RH, Ho E. Sulforaphane inhibits histone deacetylase activity in BPH-1, LNCaP and PC-3 prostate epithelial cells. *Carcinogenesis* 2006;27:811–9.
- Choi S, Lew KL, Xiao H, et al. D,L-Sulforaphane-induced cell death in human prostate cancer cells is regulated by inhibitor of apoptosis family proteins and Apaf-1. *Carcinogenesis* 2007;28:151–62.
- Xu C, Shen G, Chen C, Gelinas C, Kong AN. Suppression of NF-kappaB and NF-kappaB-regulated gene expression by sulforaphane and PEITC through IkkappaBalpha, IKK pathway in human prostate cancer PC-3 cells. *Oncogene* 2005;24:4486–95.
- Herman-Antosiewicz A, Johnson DE, Singh SV. Sulforaphane causes autophagy to inhibit release of cytochrome c and apoptosis in human prostate cancer cells. *Cancer Res* 2006;66:5828–35.
- Taylor WR, Stark GR. Regulation of the G<sub>2</sub>/M transition by p53. *Oncogene* 2001;20:1803–15.
- Rozaan LM, El-Deiry WS. p53 downstream target genes and tumor suppression: a classical view in evolution. *Cell Death Differ* 2007;14:3–9.



29. Widrow RJ, Laird CD. Enrichment for submitotic cell populations using flow cytometry. *Cytometry* 2000;39:126–30.
30. Herman-Antosiewicz A, Singh SV. Checkpoint kinase 1 regulates diallyl trisulfide-induced mitotic arrest in human prostate cancer cells. *J Biol Chem* 2005;280:28519–28.
31. Hunter T. Braking the cycle. *Cell* 1993;75:839–41.
32. Molinari M. Cell cycle checkpoints and their inactivation in human cancer. *Cell Prolif* 2000;33:261–74.
33. Boutros R, Dozier C, Ducommun B. The when and wheres of CDC25 phosphatases. *Curr Opin Cell Biol* 2006;18:185–91.
34. Pines J, Hunter T. Human cyclins A and B1 are differentially located in the cell and undergo cell cycle-dependent nuclear transport. *J Cell Biol* 1991;115:1–17.
35. Sherwood SW, Rush DF, Kung AL, Schimke RT. Cyclin B1 expression in HeLa S3 cells studied by flow cytometry. *Exp Cell Res* 1994;211:275–81.
36. Widrow RJ, Rabinovitch PS, Cho K, Laird CD. Separation of cells at different times within G2 and mitosis by cyclin B1 flow cytometry. *Cytometry* 1997;27:250–4.
37. Hendzel MJ, Wei Y, Mancini MA, et al. Mitosis-specific phosphorylation of histone H3 initiates primarily within pericentromeric heterochromatin during G2 and spreads in an ordered fashion coincident with mitotic chromosome condensation. *Chromosoma* 1997;106:348–60.
38. Gurley LR, D'Anna JA, Barham SS, Deaven LL, Tobey RA. Histone phosphorylation and chromatin structure during mitosis in Chinese hamster cells. *Eur J Biochem* 1978;84:1–15.
39. Paulson JR, Taylor SS. Phosphorylation of histones 1 and 3 and nonhistone high mobility group 14 by an endogenous kinase in HeLa metaphase chromosomes. *J Biol Chem* 1982;257:6064–72.
40. Ajiro K, Nishimoto T, Takahashi T. Histone H1 and H3 phosphorylation during premature chromosome condensation in a temperature-sensitive mutant (tsBN2) of baby hamster kidney cells. *J Biol Chem* 1983;258:4534–38.
41. Guo XW, Th'ng JP, Swank RA, et al. Chromosome condensation induced by fostriecin does not require p34cdc2 kinase activity and histone H1 hyperphosphorylation, but is associated with enhanced histone H2A and H3 phosphorylation. *EMBO J* 1995;14:976–85.
42. Matsuoka S, Huang M, Elledge SJ. Linkage of ATM to cell cycle regulation by the Chk2 protein kinase. *Science* 1998;282:1893–7.
43. Melchionna R, Chen XB, Blasina A, McGowan CH. Threonine 68 is required for radiation-induced phosphorylation and activation of Cds1. *Nat Cell Biol* 2000;2:762–5.
44. Yang J, Yu Y, Hamrick HE, Duerksen-Hughes PJ. ATM, ATR and DNA-PK: initiators of the cellular genotoxic stress responses. *Carcinogenesis* 2003;24:1571–80.
45. Hu R, Hebbar V, Kim B, et al. *In vivo* pharmacokinetics and regulation of gene expression profiles by isothiocyanate sulforaphane in the rat. *J Pharmacol Exp Ther* 2004;310:263–71.
46. Chiao JW, Chung FL, Kancherla R, Ahmed T, Mittelman A, Conaway CC. Sulforaphane and its metabolites mediate growth arrest and apoptosis in human prostate cancer cells. *Int J Oncol* 2002;20:631–6.
47. Wang L, Liu D, Ahmed T, Chung FL, Conaway CC, Chiao JW. Targeting cell cycle machinery as a molecular mechanism of sulforaphane in prostate cancer prevention. *Int J Oncol* 2004;24:187–92.
48. Shen G, Xu C, Chen C, Hebbar V, Kong AN. p53-independent G<sub>1</sub> cell cycle arrest of human colon carcinoma cells HT-29 by sulforaphane is associated with induction of p21<sup>CIP1</sup> and inhibition of expression of cyclin D1. *Cancer Chemother Pharmacol* 2006;57:317–27.
49. Jakubikova J, Sedlak J, Mithen R, Bao Y. Role of PI3K/Akt and MEK/ERK signaling pathways in sulforaphane- and erucin-induced phase II enzymes and MRP2 transcription, G<sub>2</sub>/M arrest and cell death in Caco-2 cells. *Biochem Pharmacol* 2005;69:1543–52.
50. Pham N, Jacobberger JW, Schimmer AD, Cao P, Gronda M, Hedley DW. The dietary isothiocyanate sulforaphane targets pathways of apoptosis, cell cycle arrest, and oxidative stress in human pancreatic cancer cells and inhibits tumor growth in severe combined immunodeficient mice. *Mol Cancer Ther* 2004;3:1239–48.